Journal of Innovative Optical Health Sciences
Vol. 3, No. 4 (2010) 235–245

DOI: 10.1142/S1793545810001106

A NOVEL TIME-SHARED FLUOROMETER GIVES THE MITOCHONDRIAL REDOX STATE AS THE RATIO OF TWO COMPONENTS OF THE RESPIRATORY CHAIN OF THE ANIMAL AND HUMAN BUCCAL CAVITY WITH QUANTITATIVE MEASURES OF THE REDOX ENERGY STATE

BRITTON CHANCE*,‡, SHOKO NIOKA*, A. QUO* and JENQ-RUEY HORNG†
*University of Pennsylvania
Philadelphia, PA 19104, USA
†South Taiwan University
1 Nantai Road, Yong Kang, Tainan 71005, Taiwan
‡Chance@mail.med.upenn.edu

The source of energy for life is the tissue mitochondria and they demand a complex chain of biochemicals to ensure proper physiological function. Classically, the blood levels, and not the tissue levels of these metabolites, are determined by expensive and time-consuming biochemical analyses. Since the tissue mitochondria are the consumers of the substrates of glycolysis and of fatty acid metabolism, their redox state is a unique accessible monitor of tissue metabolism and its blockade due to toxins.

Keywords: Redox state; mitochondria; optical methods; fluorometer.

1. Introduction

We have constructed two devices to monitor the metabolic states of mitochondria through their NADH and flavoprotein components in the human buccal cavity mucosa. The mitochondrial information reflects one's metabolic "well being" that can be applied to health, chronic and systemic diseases. This concept of monitoring "Well being" through mitochondrial energy states, has never been tested before. Technically, only the optical methods involve sufficiently compact instrumentation to permit noninvasive telemetric measurement of mitochondrial signals as set forth here. We target the buccal cavity mucosa — the oral cavity has been subjected to many optical studies of tissue "autofluorescence" — mainly mitochondrial NADH,[1,2] in cancer-related perturbations of the mitochondrial state.

1.1. *Dietary therapy*

Diet directly controls mitochondrial energy metabolism, and influences its membrane potential and redox states.[3]

1.2. *Hypoxia and respiratory toxins*

The mitochondria provide an oxygen sensor over 190 times more sensitive than the blood oximeter — a meaningful local tissue signal of anoxia and response to lung disease and respiratory toxins as well, particularly under the stresses of exhaustion in exercise or organ failure.

1.3. *Diseases stresses*

Mitochondrial signals from the human buccal cavity afford a novel and unique window to the redox state of metabolism, for example due to insulin

resistance.[4–8] And it may shed light on the energy metabolism of the human body under starvation and exercise stresses.[9]

The "Metabolometer" will record the mitochondrial redox states that can be altered by many substrates — normal food intake, for which glucose, alcohol and fat BHOB have different couplings to mitochondria Oxidative Phosphorylation (glucose Complex I and fat Complex II). Also, intake of toxic agents, some therapeutic agents and oxygen therapy, hypoxia or free radicals alter mitochondrial redox states systemically.[10–16]

Our technology, based upon quantitative redox state measurements by the ratio of NADH and FAD, makes the "Metabolometer" suitable for telemetered output from the human buccal mucosa, and is validated by pure chemicals and by yeast and small animal models, whose mitochondria contain the same amounts of Flavoprotein and NADH as that in the human body tissues.

Mitochondrial redox states are responsive to the body energetic function, to organ dysfunction, to the adequacy of substrates and oxygen, and to the presence of toxic substances. Thus, metabolometer gives vital information for metabolic diseases, such as diabetes, as it will indicate mitochondrial activity and alterations of glucose metabolism. Hydroxy-butyric acid (HBA) is known to reduce mitochondrial redox state, and is used as a therapeutic diet for neurodegenerative diseases (AD, PD), spinal cord injury, epilepsy, and stroke, as well as oral cancer, wound healing, and infectious diseases.[10–17] Thus, we will be able to give novel insights into their mechanism by "Metabolometer" indications.

Here we propose a noninvasive measure of "well being" from the mitochondrial energy states. The mitochondrial energy states are measured by the ratio of the NADH (Nicotinamide adenine dinucleotide) and Flavoprotein or FAD (Riboflavin 5′-adenosine diphosphate), both of which are intrinsic components of the mitochondrial electron transport chain.[18]

The fluorescence signals indicate trends of the whole body metabolic state over time and of the mitochondrial capability to produce energy from oxygen, food, and to respond sensitively to a glucose challenge and physical exercise, as validated by yeast and gerbil models. The device can be used from neonates to geriatric populations, in any set of conditions, in the hospital as well as in homecare environment.

Mitochondria are sensors of biochemical signals of the body; they are responsive to the change in levels of the most important biochemicals, such as oxygen, foodstuffs, toxins, etc., and to some hormones as delivered by the bloodstream to the buccal cavity.

1.4. *Choice of the buccal cavity*

While the NIR wavelengths are readily transmitted through the skin, the near ultra-violet wavelengths needed to excite the fluorescence of NADH are not. However, we have obtained NADH fluorescence signals from most of the exposed body organs.[19–22] Many papers have been published using the oral cavity, of which the buccal cavity is an important part.

1.5. *Comparison of the pulse oximeter and the metabolometer*

Both are responsive to O_2, but the mitochondria are over 100 fold more sensitive [$K = <10^{-9}$ M (Schindler Ref.)]. Dangerously low values as given by the pulse oximeter are indicative of Bohr's O_2 gradient and low values as given by the pulse oximeter are indicative of those at which mitochondrial cytochrome oxidase can still operate. Hemoglobin has a relatively low oxygen affinity (micromolar) and cytochrome oxidase has an extremely high oxygen affinity which may be sufficient for ATP generation. So the mitochondria are key indicators of the real tissue oxygen sufficiency for ATP production. However, the tissue O_2 gradient depends upon the respiratory rate, and the tissue O_2 gradient in the mitochondria may vary widely from rest to activity and in different organs.[23]

1.6. *Electronic developments*

There have been many attempts to measure the redox state of mitochondria of the buccal cavity of animals and humans; location into the buccal cavity requires an ingenious miniaturization that depends critically upon solid state electronics.

1.6.1. *Circuit design*

The ratio circuit for NADH and flavoprotein has a channel for each signal and takes their ratio by (1) converting to logarithms subtraction, and outputting the logarithm; or (2) digitizing and

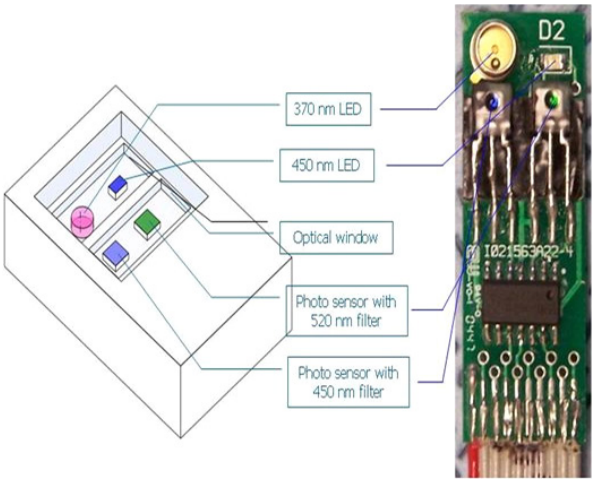

(a)

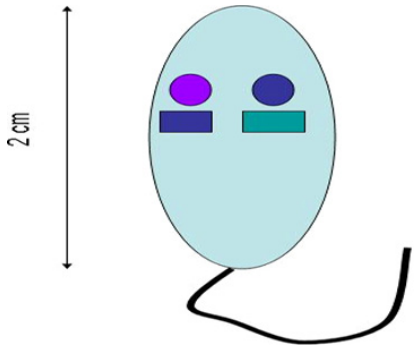

(b)

Fig. 1. (a) Circuit board construction of analogue "Metabolometer" used in the following tests with attached identification of the circuit elements. (b) Proposed surface view of the 2-cm capsule showing the two LED sources and small detectors protected by green and blue gelatin filters with string attached for retrieval.

dividing in the software. The analog circuit shown in Fig. 1 has been designed, constructed and tested at the University of Pennsylvania. This is a novel dual-wavelength, time-shared fluorometer ("Metabolometer") for readout directly (wired) or by telemetry of NADH and flavoprotein signals. Instrumental simplicity is required for an indwelling wearable low cost instrument with telemetered (in the case of neonates-wired) readout. The sensitivity has been tested using a yeast model providing mitochondrial redox states 1 to 5.

1.6.2. *Calibrations and animal tests*

The proposed tests include calibrations based upon pure NADH and flavoprotein solutions, cells (yeast) with blood phantoms and with small and large animal models.[24,25] Adults and juveniles are to be studied for effects of exercise and food, especially glucose and ketone.[26] We can also monitor exceptional exercises (Iron Man, triathlon).

2. Metabolometer Design

The electronic engineering designs of Figs. 1 and 2 consist of 450 nm and 370 nm LEDs flashed alternatively for 10 msec. Attached thereto at a distance of 3 mm but protected by green and blue gelatin filters, respectively at 520 nm and 450 nm, are two Si diode detectors followed by current-to-voltage conversion and sample and hold detection into a one-sec time constant with logarithmic conversion, and signal subtraction for signal ratioing and telemetering. Digital conversion after the preamplifier may facilitate ratioing, telemetering, and digital signal processing using wired output for the gerbil model. In the human subject model, more space is available and the ratioed signals can be telemetered to a remote indicator and digital recorder.

In collaboration with South Taiwan University, we have miniaturized the design of Fig. 2 within the dotted region into a very small capsule (Fig. 3) with wired connections to the remainder of the circuit. The wireless version will be encased in a larger capsule for adult telemetry of the signals to the log convertor. Subtractor and digital voltmeter are as shown in Fig. 2.

A waterproof transparent plastic capsule (Ultra-mold, Yardley, PA) of 2.5 cm diameter and 5 mm thickness will be made for the electronic components (Fig. 3) as miniaturized by Prof Horng of South Taiwan University.

2.1. *Optical filter size*

Since we are dealing with multiply scattered light for signal detection, the detector area can be varied by the choice of detector from 1 to 100 mm squared with a corresponding increase of signal, without an increase in the circuit board area, only thickness to accommodate a second 2 by 2 cm "detector" circuit board.

2.2. *Ratiometric measures*

The fact that here we propose that the measurement of the ratio of two essential components of the mitochondrial electron transport chain affords possibilities for quantization which is not available for cytosolic enzymes, for which ratiometric measures (independent of the number of

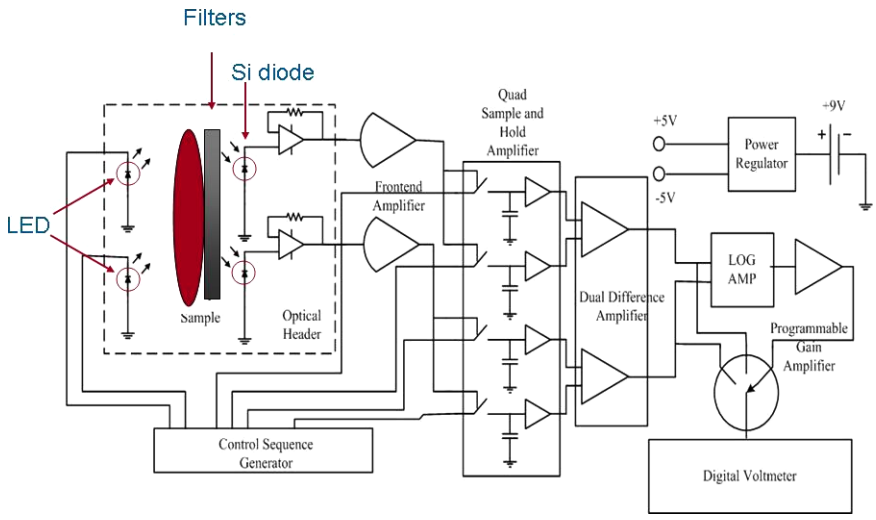

Fig. 2. Circuit diagram of prototype "Metabolometer" for the infant, showing timing generator with LEDs as light sources, filtered detectors, amplifiers, as in the dashed rectangle with separated sample and hold detectors, log conversion and subtraction for ratio detection with digital display. An alternative design is digitized immediately after the optical preamp with ratio conversion, DSP and output to a DVM and recorder.

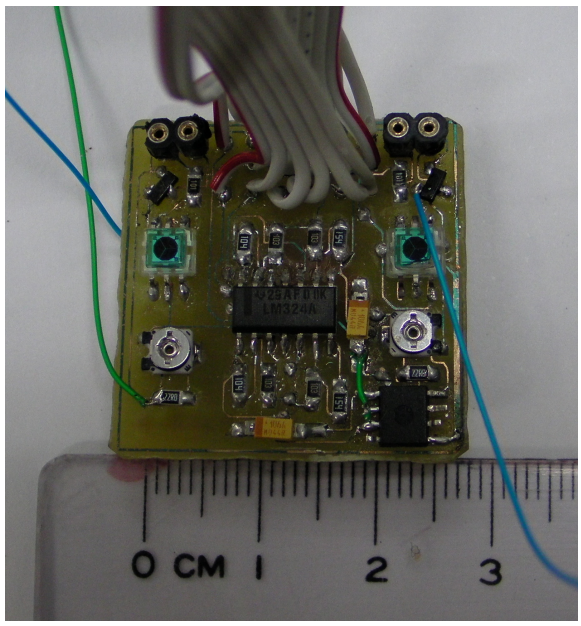

Fig. 3. The present construction of the time-shared microchip metabolometer with small Si diode detectors and sample and hold detection at STU by Prof Horng to be encased in a plastic envelope and used in the yeast calibration, future Huskie study by Dr M. Davis and, with IRB approval, in human subjects.

mitochondria) are indicative of the redox ratio of many substrate couples, for example, Lactate/pyruvate and BHOB/acetoacetate.[31] In addition, the redox state of the buccal tissue, like that of many other tissues studied, shows a significant redox change in the transition from normoxia to anoxia (States 3 to 5) and will be expected to show a similar large transition in the starved to fed state caused by glucose addition (States 2 to 3). The States 2 to 3 are the feeding response, while the States 3 to 5 transition in Fig. 5 may not be available for human subjects, taking note that the "Gold Standard" is the pure chemicals (see below under calibration). However, the value of the ratio at any time is an important health index for human subjects.[24,27–31]

2.3. *Current design of STU*

By judicial use of microelectronics, the metabolometer has been reduced in size to 2.4 by 2.4 cm and enclosed in a plastic envelope; it is suitable for the adult buccal cavity.

3. Test Results

Sensitivity, HbO_2 crosstalk, and calibration methods with yeast blood model gives the signal-to-noise ratio of NADH and Fp measurement with a yeast blood model. Baker's yeast mitochondria have the same NADH and flavoprotein signals and metabolic behavior as those in animal tissue, justifying our proposal to use Baker's yeast as a model. It is well recognized that cytosolic NADH is present in yeast and it is distinguished from mitochondrial NADH signal by the flavoprotein signal. Crosstalk due to hemoglobin absorption is re-evaluated using the yeast model.

3.1. *Preparation of the standard solution of NADH and FAD for the "Metabolometer"*

To establish the calibration curves of NADH (reduced disodium salt) and FAD (disodium salt), two sets of standard solution were prepared by weighing the appropriate amount of NADH and FAD salt (Sigma Aldrich). The NADH will be diluted with 10 mM Tris-HCl buffer with pH = 8.5 and FAD powder will be diluted with Hanks balanced salt. The NADH and NAD stock solution concentration can be determined to be around 1 mM (UV-Vis spectrometer). Four solutions of various concentrations of NADH or FAD will be prepared by serial dilution with 1% intralipid, which mimics a normal tissue scattering. These are eight standards of NADH and FAD and a Tris-HCl buffer.[24,25]

3.2. *Preparation of yeast model and measurement of mitochondria metabolic states*

We use a model consisting of a 1,000-ml rectangular vessel made of plastic containing up to 20% by weight baker's yeast, which contains abundant mitochondria and a high scattering coefficient. The tank is fitted with oxygen, nitrogen and a sparger, placed on a stirrer with temperature adjustment equipment (25°C) and a pH meter (may be pH 5 or 6); oxygen electrode will be monitored at all times. Yeast suspension is prepared a day before to provide State 2 by overnight sparging with O_2 and State 5 is readily obtained by sparging with N_2.

Calibration of the "Metabolometer" in each test will also be done using the solutions described above before and after each experiment.

The following transitions of mitochondrial activities are readily measured by changes in Fp/NADH:

(1) State 3 transition from State 2 with substrates of mitochondria. We will add 10 mM glucose and/or ethanol to obtain State 3. The acid (HBA, Lactate and Succinate) will not cross the yeast cell membrane. State 3 to 3u, Dinitrophenol (DNP), or pentachlorophenol (PCP) will cause mitochondrial uncoupling mimicking apoptosis as caused by some anti-cancer drugs for State 3u measurement.
(2) State 5 hypoxia/anoxia study (from States 2 and 3 to State 5). After a proper substrate injection, States 3 to 5 transitions to anaerobiosis will occur due to yeast respiration even without N_2 sparging.
(3) State 5 mitochondrial toxicity study (States 3 to 5 but occurring in the presence of O_2). We will use mitochondrial inhibitors, rotenone, amytal (Complex I), antimycin (Complex III), and oligomycin (Complex V) to cause State 5.

3.3. *Crosstalk of hemoglobin and redox states*

The yeast model will contain blood at physiological concentration and crosstalk will be quantitated in the hypoxia-induced States 3 to 5 transition.

3.4. *Fluorescence of mitochondrial NADH and flavoprotein*

The fluorescence emission spectra from isolated mitochondria in the UV and Visible spectra of NADH and flavoprotein show that their signals overlap in that the excitation of flavoprotein overlaps with the emission of NADH instead of attempting to spectroscopically isolate the two. We have designed a time-sharing fluorometer to respond sensitively to the metabolic states of the two pigments by time-sharing the two excitation wavelengths. The emission spectrum of isolated mitochondria is shown in Fig. 4. NADH signal is high in State 4 and less in States 3 and 2 while conversely FAD signal is low in State 4 and increases in State 3. Since the increase in the rate of metabolism causes the change from State 4 to 3, we have an indicator of metabolic activity (a metabolometer).

3.5. *Metabolic states*

There are five metabolic states of mitochondria that are of great importance in normal and pathological functions of the body. They are summarized below as a guide in human subject diagnostics.[32–41]

The metabolic states of mitochondria were defined by Chance and Williams (1955) and are listed below:

State 2. A metabolically substrate depleted state due to ADP supplement causing highly oxidized carriers and even more oxidized in the uncoupled State 3u.
State 3. The actively metabolizing state with excess substrate and ADP and with ATP synthesis. The carriers are oxidized, but not as far as in State 2.

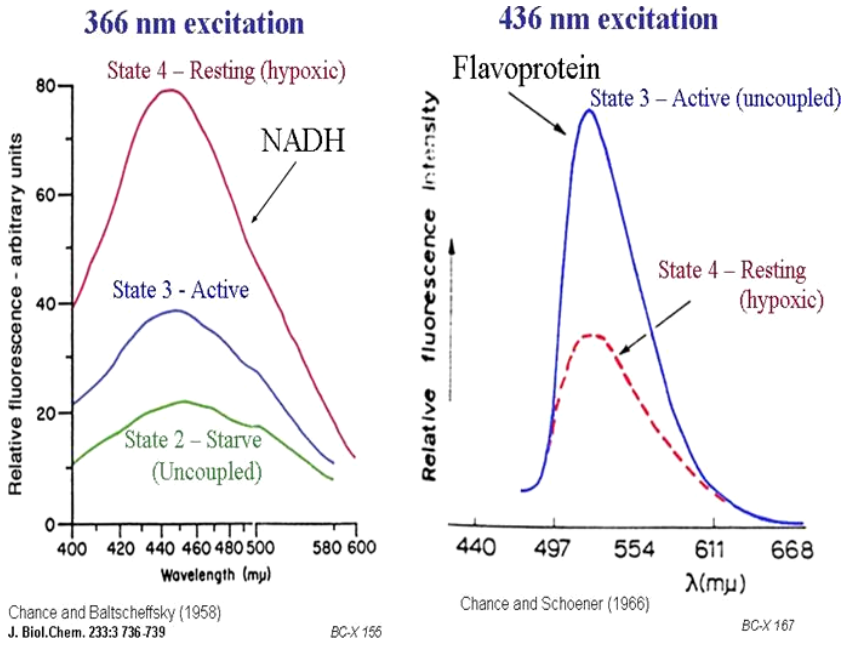

Fig. 4. Fluorescence emission spectra of mitochondrial NADH (left) and flavoprotein (right) with 366 nm and 436 nm excitation, respectively, of suspensions of isolated mitochondria in different redox States 2, 3, 4 for NADH and 3 and 4 for flavoprotein, illustrating the great sensitivity of the NADH/flavoprotein ratio to metabolic activation in the States 4 to 3 transition.[41] Anaerobiosis maximizes NADH and minimizes flavoprotein signals.

State 3u. Occurring with the presence of an uncoupler[26,42] or with apoptosis loss of membrane potential induced by drug therapy and more oxidized than in State 3.[36]

State 4. The metabolically resting state due to the lack of ADP, and the presence of substrate. The carriers are reduced as shown in Fig. 4.

State 5. The hypoxic state due to lack of tissue O_2 or to the presence of toxic agents. Carriers are highly reduced beyond the State 4 level, as in Fig. 4.

State 6. A Ca-blocked state with carriers highly oxidized.[43]

3.6. *Hemoglobin interference*

Since the absorption bands of oxy- and deoxyhemoglobin overlap with the spectra of Fig. 4, some interference is expected and the data of Fig. 4 show that the effect upon the ratio of NADH and flavoprotein is very small and is quantified as follows.

The data of Fig. 5 are the result of an intensive study of the effect of HbO_2 upon the redox ratio Fp/NADH. In these studies yeast was used at a concentration matching that of the buccal cavity and Hb was titrated up to the amounts equal to that

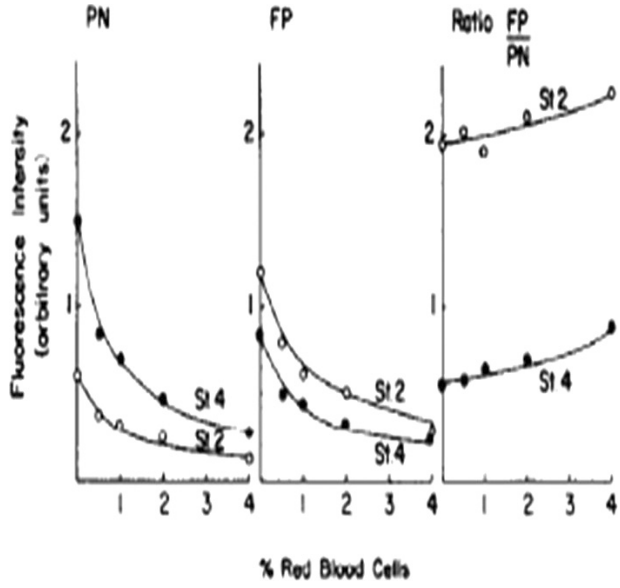

Fig. 5. The crosstalk. The crosstalk between HbO_2 and the redox state, FP/PN. Addition of increasing amounts of HbO_2 to a highly scattering yeast cell suspension maintained aerobically by sparging with O_2.

in the blood vessels and the effect upon the redox ratio was recorded as in the figure. It is clear that while Fp and NADH alone are reduced significantly by the absorption of blood, the ratio is only slightly increased. This is due to the fact that the absorption of Hb affects NADH and Fp almost equally and

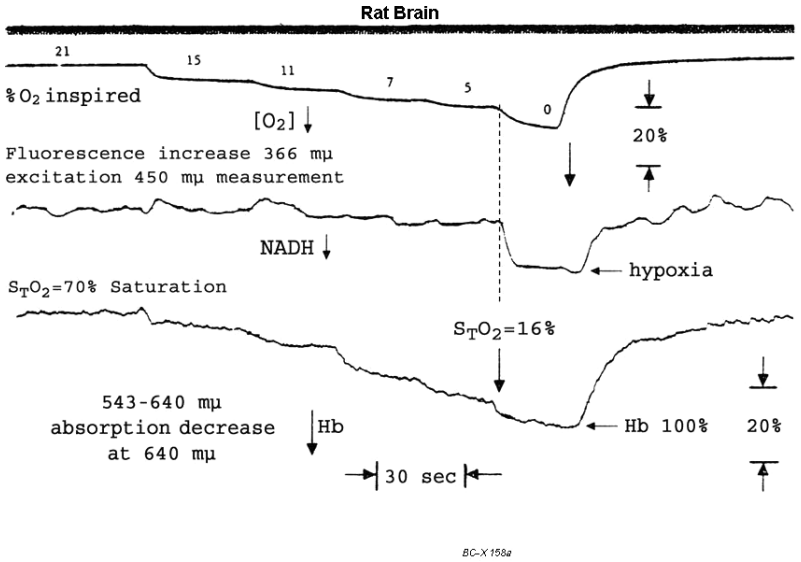

Fig. 6. A rat brain study. Correlation of the inspired oxygen (top trace), the redox state of NADH (middle trace) and the deoxygenation of physiological amounts of hemoglobin (5%) (bottom trace). The dashed vertical line indicates the critical oxygen concentration (16%) for brain mitochondrial function — a pulse oximeter would give a value of 16%. The abrupt change in the NADH trace is a mitochondrial warning of hypoxic death.[28,35]

makes it unnecessary to provide any compensation for Hb in the design of Fig. 3 in accordance with the recordings *in vivo* of Figs. 5 and 7.

The quantitative detection of systemic hypoxia by hemoglobin desaturation is difficult. Redox signals of brain hypoxia are very robust; the "Metabolometer" not only detects the state of well being, but also warns, by the fully reduced State 5, that death will soon occur, caused by not only lack of O_2, but also many toxic agents in bland food, such as cyanide, azide, antimycin-A, rotenone, Phenobarbital, etc.,[42,43] causing State 5 and depletion of ATP.[19–21]

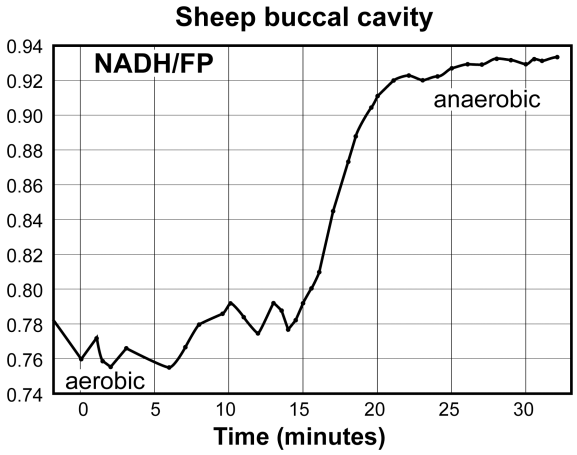

Fig. 7. Data from a sheep buccal cavity during the States 3 to 5 transitions. We used the prototype device (Fig. 2) giving the ratio of the NADH and FAD fluorescent signals. We show that hypoxia increases the NADH/flavoprotein ratio from 0.76 to 0.94 or decreases the ratio of Fp/NADH by a factor of 1.24.

4. Large Animal Models: Sheep and Huskies

4.1. *Studies of sheep*

We have used the sheep buccal cavity with the prototype device, and conducted a hypoxia study (Fig. 7). The response of the device to the standard normoxia to anoxia transition test for mitochondrial function is shown. The sheep, under appropriate animal subject protocol, was anesthetized with breathing isofluorane to avoid a change of mitochondrial steady state as with nembutal and anesthesia was ensured by standard test. Hypoxia was caused by breathing N_2. At minutes 6 to 10, there is a small crosstalk signal due to the early deoxygenation of hemoglobin. At minute 14 the tissue P_{O_2} reached the critical point less than nanomolar of the inspired gas, and the redox value increased from 0.76 to 0.94 with very good signal-to-noise ratio — greater than 10 to 1. The calculation of Delta requires calibrations described above. Thus the tissue redox fluorometry gives the critical P_{O_2} for tissue mitochondrial function as contrasted with hemoglobinometry as measured by the finger pulse oximeter rNelcor.

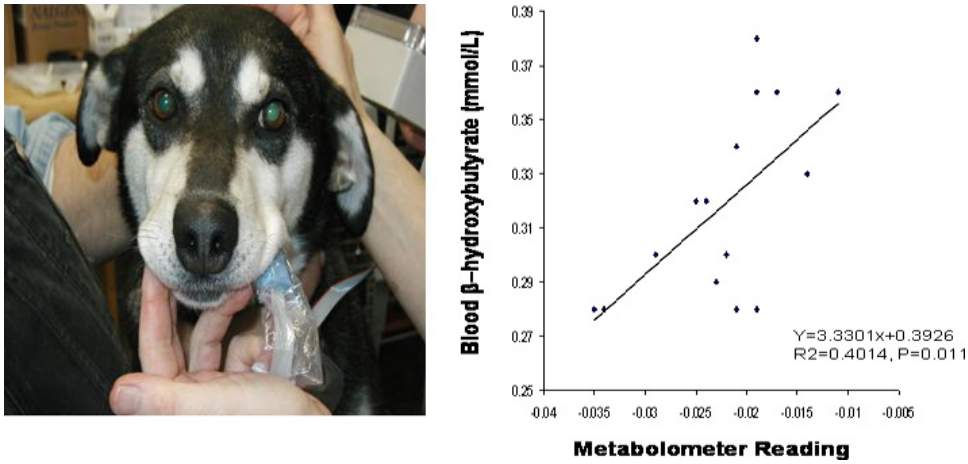

Fig. 8. Using the prototype metabolometer of Fig. 2, enveloped in plastic envelope, on the sled dogs. Fifteen dogs were tested for their buccal cavity mitochondrial redox states at rest intervals and at the end of each of the 5-day run. Metabolometer readings were positively correlated with whole blood ketone measurements ($R^2 = 0.40$, $p = 0.011$).

The effect of toxins such as azide, antimycin, rotenone, barbiturates, etc, on the yeast and animal models will also cause a States 3 to 5 transition and ATP loss similar to results of Fig. 7 and of previous studies on NADH only.[19–21,42,43] Ratiometric data, NADH/Fp, will quantify the redox states more accurately. These data will provide calibrated absolute values of redox state measurements for the first time rather than uncalibrated changes of those fluorescence signals.[1,2,10–13]

4.2. *Studies of Huskies*

Dr M. Davis has kindly compared biochemical assay of blood with the signals from an early model of the metabolometer (Fig. 2) and is currently testing the administration of BHOB on Alaska Sled Dogs (see Fig. 8) before exercise ($N = 15$). In the Ididerod dog sled race across Alaska, the sled dogs will use up all their glycogen storage within two days (240 miles) of running, and from the 3rd day to the finish, they rely on fatty acids (BHOB) as a mitochondrial fuel (Fig. 8). The dogs were not sedated and, as the picture shows, the metabolometer was not securely located in the different dogs' buccal cavity and there is significant scattering in the data because of the difficulty to obtain dog blood samples under the rigorous conditions of Ididerod where two tests showed no increase in BHOB. Nevertheless, an average of three-fold increase of redox state between BHOB concentration and mitochondrial redox states in the buccal cavity of dogs is shown, with an average $R^2 = 0.40$ and $p = 0.011$. The studies will be continued with the more advanced miniature circuit of Fig. 3.

5. Human Subject Studies

5.1. *Actinic effects–NADH*

While detailed and monitored perturbative studies have been published to occur over 45 min illumination with the 1-KW high pressure Hg arc, many studies of NADH fluorescence of the oral cavity with a variety of excitation light sources and powers near 340 nm, the excitation peak, have been recently surveyed, as well as Mayevsky multi-element fiber coupled "optoelectrode" for the human brain. Thus ready IRB approval is expected.

Two of the authors (BC and JRH) have calculated that the intensity of the time-shared LED at the 370 nm wavelength as compared to the high intensity Hg arc at 370 nm, which gave minor effects.[35] Taking into account the reduced absorption of NADH at 370 nm and the low power of the LED, these would lead to a high degree of safety from actinic effects even over long exposure times as is expected for exercise stresses where battery economy would require activation of the metabolometer on a duty ratio of 10%.

5.2. *The danger of swallowing*

The telemetered metabolometer is mitigated by the string attached to the telemetered version as shown in Fig. 2; Fig. 3 shows a wired version which has no danger of being swallowed.

5.3. *Current status technical*

The current 1 mm × 1 mm "RGB" detectors will be upgraded by the 1 cm^2 Thor 1010 Si diodes with Wratten 47 and 61 Gelatin filters and 3 LED excitation of both wavelengths, to eliminate the preamplifier and to increase the S/N with only an increase in thickness of the sensor.

5.4. *Experimental studies*

A yeast model has been constructed and is under test. Two human subjects have volunteered to test the plastic enclosed unit of Fig. 3 with no discomfort and signals of 100 and 60 mv for NADH and flavoprotein from their buccal cavities and an increase of 100-fold with the Thor 1 cm^2 Si diode detectors.

6. Discussion

6.1. *Human subject studies*

The obtaining of significant human buccal cavity signals from two normal subjects will be followed with detector improvements and yeast model tests and buccal cavity tests, and will be used under IRB approval, in glucose response in normal and diabetic subjects and in exercise studies.

6.2. *Mitochondrial signaling of apoptosis-response to therapeutics*

For a buccal or sublingual cancer, in cancer therapy with anticancer drugs that cause apoptosis (cisplatin, etc), an uncoupled, open pore state, and, if systemically delivered, the buccal cavity mitochondria will be affected as well, serving as an immediate biomarker of the effectiveness of cancer therapy in causing apoptosis of the buccal cavity. In fact, the deleterious effect of anticancer and indeed other drugs upon body energy resources will also be mirrored in the oxidation of the redox state of the buccal cavity mitochondria from the normal States 3 to 3u.

6.3. *Sites of clinical studies*

IRB approval will be sought at the National Cheng Kung University (NCKU) and at University of Pennsylvania [HUP (Penn)] hospitals, where NIR breast cancer studies are currently in progress. The following studies will be conducted: 50 studies in diabetic patients and in 10 subjects under cancer therapy of the buccal cavity, 20 studies of juvenile ketosis in CHOP, and 20 studies of exercise exhaustion in long distance runners at Penn athletics. The two latter studies will also be done at South Taiwan University hospital and will include athletics such as "Football" and "Iron man".

7. Conclusions

The buccal cavity "Metabolometer" will monitor the blood delivery of all substrates and toxins and evaluate the mitochondrial "function or dysfunction" in the buccal cavity to the activity of the glycolytic, lipid and CAC pathways that deliver reducing substances to sites 1 and 2 of the tissue mitochondria, It will be used to detect any pathologies either in delivery or consumption of reducing and oxidizing equivalents by the mitochondria or the presence of toxic substances. The impact of site 2 substrates upon the site 1 redox state can also be monitored by inhibition of "reversed electron transfer". Thus, all normal and defective functions of mitochondria in response to the above blood deliveries as well as the levels of substrates delivered by the glycolytic and citric acid cycle enzymes will be detected by comparing the mitochondrial redox states to those of the normal subjects. The evaluation applies to all blood borne drugs as well as the therapeutic impact of hydroxybutyric acid (HOB) used to treat epilepsy, Alzheimer's disease, Parkinson's diseases as well as the toxic effects of high levels of drugs such as aspirin, which is used to treat stroke, heart disease, and ketosis caused by diabetes.

Appendix

Abbreviations

HBA: Hydroxybutyric acid

LED: light emitting diode

SiD: silicon diode detector

SH: Sample and hold detector

DSP: Digital signal processing [includes analog to digital convertor]. This circuit normalizes the signal and takes their ratio on a 0-to-1 scale and sets the repetition rate according to the signal change. Telemeter sends out the ratio to a nearby radio receiver for data signal processing, display, recording.

Draft IRB application

(1) A noninvasive optical device for quantifying the tissue redox states
(2) The metric is the ratio of the intensity of two natural fluorochromes of the tissue
(3) The two wavelengths used are 470 and 370 nm
(4) The possible actinic effects are minimized by a peak power of 60 mwatt sec and an average power of 0.1 mwatt sec as compared with the ANSI regulation of mwatt sec
(5) The capsule is coated with a nontoxic, insoluble sealant suitable for 10 min residence time in the buccal cavity every 3 hours
(6) A pair of Pt electrodes 1 mm apart and polarized at 0.1 volt ensures that the capsule is in contact with saliva and in case of rupture
(7) The detectors contain two Si diodes followed by current-to-voltage conversion and the LED contains two wavelengths. Both are sealed in the capsule and not water accessible in the case of failure of the warning of the rupture of the capsule.

References

1. S. McGee, J. Mirkovic, V. Mardirossian, A. Elackattu, C. C. Yu, S. Kabani, G. Gallagher, R. Pistey, L. Galindo, K. Badizadegan, Z. Wang, R. Dasari, M. S. Feld, G. Grillone, "Model-based spectroscopic analysis of the oral cavity: Impact of anatomy," *J. Biomed. Opt.* **13**(6), 064034 (2008).
2. W. Zheng, Y. Wu, D. L. Li, J. Y. Q., "Autofluorescence of epithelial tissue: Single photon versus two-photon excitations," *Biomed. Opt.* **13**, 15410–208 (2008).
3. K. A. Kasischke, H. D. Vishwasrao, P. J. Fisher, W. R. Zipfel, W. W. Webb, "Neural activity triggers neuronal oxidative metabolism followed by astrocytic glycolysis," *Science* **305**(5680), 99–103 (2004).
4. B. Chance, G. Williams, "Respiratory enzymes in oxidative phosphorylation. VI. The effects of adenosine diphosphate on azide-treated mitochondria," *J. Biol. Chem.* **221**(1), 477–489 (1956).
5. S. Nioka, K. McCully, G. McClellan, J. Patk, B. Chance, "Oxygen transport and intracellular bioenergetics on stimulated cat skeletal muscle," *Adv. Exp. Med. Biol.* **510**, 267–272 (2003).
6. B. Yerby, R. Deacon, V. Beaulieu, J. Liang, J. Gao, D. Laurent, "Insulin-stimulated mitochondrial adenosine triphosphate synthesis is blunted in skeletal muscles of high fat fed rats," *Metabolism* **57**(11), 1584–1590 (2008).
7. M. A. Abdul-Ghani, R. A. DeFronzo, "Mitochondrial dysfunction, insulin resistance, and type 2 diabetes mellitus," *Curr. Diab. Rep.* **8**(3), 173–178 (2008).
8. M. A. Abdul-Ghani, F. L. Muller, Y. Liu, A. O. Chavez, B. Balas, P. Zuo, Z. Chang, D. Tripathy, R. Jani, M. Molina-Carrion, A. Monroy, F. Folli, R. H. Van, R. A. DeFronzo, "Deleterious action of FA metabolites on ATP synthesis: Possible link between lipotoxicity, mitochondrial dysfunction, and insulin resistance," *Am. J. Physiol. Endocrinol. Metab.* **295**, E678–85 (2008).
9. M. Bassami, S. Ahmadizad, D. Doran, D. P. MacLaren, "Effects of exercise intensity and duration on fat metabolism in trained and untrained older males," *Eur. J. Appl. Physiol.* **101**(4), 525–532 (2007).
10. S. T. Henderson, "Ketone bodies as a therapeutic for Alzheimer's disease," *Neurotherapeutics* **5**(3), 470–480 (2008).
11. C. M. Studzinski, W. A. MacKay, T. L. Beckett, S. T. Henderson, M. P. Murphy, P. G. Sullivan, W. M. Burnham, "Induction of ketosis may improve mitochondrial function and decrease steady-state amyloid-beta precursor protein (APP) levels in the aged dog," *Brain Res.* **1226**, 209–217 (2008).
12. M. A. Puchowicz, J. L. Zechel, J. Valerio, D. S. Emancipator, K. Xu, S. Pundik, J. C. LaManna, "Lust, W. D. Neuroprotection in diet-induced ketotic rat brain after focal ischemia," *J. Cereb. Blood Flow Metab.* **28**(12), 1907–1916 (2008).
13. W. T. Plunet, F. Streijger, C. K. Lam, J. H. Lee, J. Liu, W. Tetzlaff, "Dietary restriction started after spinal cord injury improves functional recovery," *Exp. Neurol.* **213**, 28–35 (2008).
14. A. L. Hartman, M. Lyle, M. A. Rogawski, M. Gasior, "Efficacy of the ketogenic diet in the 6-Hz seizure test," *Epilepsia.* **49**(2), 334–339 (2008).
15. L. T. Zhang, Y. M. Yao, J. Q. Lu, X. J. Yan, Y. Yu, Z. Y. Sheng, "Sodium butyrate prevents lethality of severe sepsis in rats," *Shock.* **27**(6), 672–677 (2007).
16. N. Grinberg, S. Elazar, I. Rosenshine, N. Y. Shpigel, "Beta-hydroxybutyrate abrogates formation of bovine neutrophil extracellular traps and bactericidal activity against mammary pathogenic *Escherichia coli*," *Infect. Immun.* **76**, 2802–2807 (2008).
17. T. Feldkamp, A. Kribben, N. F. Roeser, R. A. Senter, S. Kemner, M. A. Venkatachalam, I. Nissim, J. M. Weinberg, "Preservation of Complex I function during hypoxia-reoxygenation-induced mitochondrial injury in proximal tubules," *Am. J. Physiol. Renal. Physiol.* **286**, F749–F759 (2004).
18. R. L. Veech, J. W. R. Lawson, N. W. Cornell, H. A. Krebs, "Cytosolic phosphorylation potential," *J. Biol. Chem.* **254**, 6538–6547 (1979).

19. B. Chance, J. R. Williamson, D. Jamieson, B. Schoener, "Properties of reduced pyridine nucleotide fluorescence of the isolated and *in vivo* rat heart," *Biochem. Zeit.* **341**, 357–377 (1965).
20. B. Chance, B. Schoener, "A correlation of absorption and fluorescence changes in ischemia of the rat liver, *in vivo*," *Biochem. Zeit.* **341**, 340–345 (1965).
21. B. Chance, B. Schoener, F. Schindler, "The intracellular oxidation-reduction state," *In Oxygen in the Animal Organism* (Dickens, F. N. ed.), Pergammon Press, London, pp. 367–388 (1964).
22. B. Chance, B. Schoener, R. Oshino, F. Itsak, Y. Nakase, "Oxidation-reduction ratio studies of mitochondria in freeze-trapped samples. NADH and flavoprotein fluorescence signals," *J. Biol. Chem.* **254**(11), 4764–4771 (1979).
23. B. Quistorff, B. Chance, A. Hunding, "An experimental model of the Krogh Tissue Cylinder: Two dimensional quantitation of the oxygen gradient. In *Oxygen Transport to Tissue — III* (Silver, I. E., Bucher, H., eds.)," Plenum Publishing Corp, NY, pp. 127–133 (1978).
24. H. N. Xu, B. Wu, S. Nioka, B. Chance, L. Z. Li, "Calibration of CCD-based redox imaging for biological tissues," *Proc. SPIE* **7262**, 72622F (2009).
25. H. N. Xu, B. Wu, S. Nioka, B. Chance, L. Z. Li, "Calibration of redox scanning for tissue samples," *Proc. SPIE* **7174**, 71742F (2009).
26. K. Sato, Y. Kashiwaya, C. A. Keon, N. Tsuchiya, M. T. King, G. K. Radda, B. Chance, K. Clarke, R. L. Veech, "Insulin, ketone bodies, and mitochondrial energy transduction," *FASEB J.* **9**, 651–658 (1995).
27. J. V. Rocheleau, W. S. Head, D. W. Piston, "Quantitative NAD(P)H/flavoprotein autofluorescence imaging reveals metabolic mechanisms of pancreatic islet pyruvate response," *J. Biol. Chem.* **79**, 31780–7 (2004).
28. N. Ramanujam, M. F. Mitchell, A. Mahadevan, S. Warren, S. Thomsen, E. Silva, R. Richards-Kortum, "*In vivo* diagnosis of cervical intraepithelial neoplasia using 337-nm-excited laser-induced fluorescence," *Proc. Natl. Acad. Sci. USA* **91**, 10193–7 (1994).
29. I. Georgakoudi, B. C. Jacobson, M. G. Müller, E. E. Sheets, K. Badizadegan, D. L. Carr-Locke, C. P. Crum, C. W. Boone, R. R. Dasari, J. Van Dam, M. S. Feld, "NAD(P)H and collagen as *in vivo* quantitative fluorescent biomarkers of epithelial precancerous changes," *Cancer Res.* **62**(3), 682–687 (2002).
30. B. Chance, "The kinetics of flavoprotein and pyridine nucleotide oxidation in cardiac mitochondria in the presence of calcium," *FEBS Lett.* **26**(1), 315–319 (1972).
31. J. V. Rocheleau, W. S. Head, D. W. Piston, "Quantitative NAD(P)H/flavoprotein auto-fluorescence imaging reveals metabolic mechanisms of pancreatic islet pyruvate response," *J. Biol. Chem.* **279**(30), 31780–7 (2004).
32. B. Chance, "Enzymes in action in living cells: The steady state of reduced pyridine nucleotide," *The Harvey Lectures Series*, New York Academic Press, Inc., pp. 145–175 (1955).
33. E. C. Slater, "Keilin, cytochrome, and the respiratory chain," *J. Biol. Chem.* **278**, 16455–16461 (2003).
34. O. Warburg, W. Christian, *Bio. Chem. Zeit.* **287**, 291–328 (1936).
35. A. Mayevsky, B. Chance, "Oxidation-reduction states of NADH *in vivo*: From animals to clinical use," *Mitochondrion.* **7**(5), 330–9 (2007).
36. B. Chance, G. Williams, "Respiratory enzymes in oxidative phosphorylation. I. Kinetics of oxygen utilization," *J. Biol. Chem.* **217**(1), 383–393 (1955).
37. B. Chance, G. Williams, "Respiratory enzymes in oxidative phosphorylation. II. Difference spectra," *J. Biol. Chem.* **217**(1), 395–407 (1955).
38. B. Chance, G. Williams, "Respiratory enzymes in oxidative phosphorylation. III. The steady state," *J. Biol. Chem.* **217**(1), 409–427 (1955).
39. B. Chance, G. Williams, "Respiratory enzymes in oxidative phosphorylation. IV. The respiratory chain," *J. Biol. Chem.* **217**(1), 429–438 (1955).
40. B. Chance, M. T. Dait, C. Chang, T. Hamaoka, F. Hagerman, "Recovery from exercise-induced desaturation in the quadriceps muscles of elite competitive rowers," *Am. J. Physiol.* **262**, C766–C775 (1992).
41. B. Chance, H. Baltscheffsky, "Respiratory enzymes in oxidative phosphorylation. VII. Binding of intramitochondrial reduced pyridine nucleotide," *J. Biol. Chem.* **233**(3), 736–739 (1958).
42. B. Chance, G. Hollunger, "Inhibition of electron and energy transfer in mitochondria. IV. Inhibition of energy-linked diphosphopyridine nucleotide reduction by uncoupling agents," *J. Biol. Chem.* **278**, 445–448 (1963).
43. B. Chance, "The energy-linked reaction of calcium with mitochondria," *J. Biol. Chem.* **240**(6), 2729–2748 (1965).